Acta Polytechnica **60**(1):1–11, 2020
DOI:10.14311/AP.2020.60.0001

PERFORMANCE ANALYSIS OF QUADRATURE CHAOS SHIFT KEYING COMMUNICATION SYSTEM BASED ON SHORT REFERENCE TECHNIQUE

Hesham Adnan Alabbasi[a], Izz Kadhum Abboud[b], Fadhil Sahib Hasan[c,*]

[a] *Mustansiriyah University, College of Education, Computer Science Department, Filastin Street, 10052 - Baghdad, Iraq*

[b] *Mustansiriyah University, College of Engineering, Computer Engineering Department, Bab Al Muadham, 10047 - Baghdad, Iraq*

[c] *Mustansiriyah University, College of Engineering, Electrical Engineering Department, Bab Al Muadham, 10047 - Baghdad, Iraq*

[*] corresponding author: fadel_sahib@uomustansiriyah.edu.iq

Abstract. One of the most famous techniques of non-coherent differential chaos shift keying (DCSK) is Quadrature chaos shift keying (QCSK) system, this system suffered from lowering the data rate and increasing the bit energy during the bit transmission even though its rate doubling the one of the DCSK. Short reference (SR) algorithm is proposed for the QCSK system to design the SR-QCSK communication system that enhances these drawbacks. The main idea of the short reference technique is minimizing the length of the reference chaotic signal (β) at a transmitter by a factor P comparing to produce R samples for the new reference signal while the length of the information-bearing signal remained unchanged, this occurs by duplicating the reference signal P times to get the same length as the conventional QCSK. Therefore, the symbol duration is reduced from 2βTc to (R+β)Tc. The data rate and energy saving improvement factor in a percent form is derived and compared with the QCSK and DCSK systems. Also, the BER analytical expression is derived for the SR-QCSK in additive white Gaussian noise and Rayleigh fading channel. The experimental simulation results proved that the theory derivation gives a good analysis tracking for the BER performance. The SR-QCSK system is compared with other DCSK techniques and the simulation results show that it has a superior performance in the multipath Rayleigh fading channel.

Keywords: DCSK, SR-QCSK, high information rate, energy saving, performance analysis, chaotic maps.

1. Introduction

During the last few years, chaotic signals became one of the techniques of interest in digital communication systems, especially in spread spectrum systems due to the sensitivity to the initial condition that allows to generate an infinite number of signals with low cross correlation between them [1], simple in design with low cost [2], having wideband continuous spectrum with a good randomness nature that increased the security of the system [3], immunity against multipath fading channels [4], resistance to jamming with a low probability of interception [5].

Chaos based digital communication systems can be designed either as coherent or non-coherent detection. In the coherent detection like chaos shift keying (CSK) system [6], the synchronization of chaotic carriers between the transmitter and receiver is required. In the non-coherent detection like differential chaos shift keying (DCSK) [4], the sending bit is recovered without the need of the channel-state information at the receiver side. For this reason, the non-coherent detection is used in the digital communication systems rather than the coherent detection.

The most popular study of non-coherent digital communication systems is DCSK that was first proposed in [7]. The approximation and Exact bit error rate analysis of DCSK over a multipath fading channel were derived in [4, 8, 9]. In the last 16 years, many studies were aimed to explore the weaknesses in the DCSK system. In [10, 11] frequency modulator FM-DCSK is used to enhance the weakness of a variant transmitter bit energy. In [12–15], quadrature chaos shift-keying, high efficiency HE-DCSK, quadrature amplitude modulation QAM-DCSK and Mary DCSK, respectively, are proposed for improving the data-rate and spectral efficiency of the DCSK system. In the QCSK, quadrature phase shift keying (QPSK) is combined with the DCSK to double the data-rate. Hilbert transform is used to create an orthogonal chaotic signal that allows transmitting two bits on the same slot. A similar scenario is used for the M-array DCSK, but with Mary Phase Shift Keying (MPSK) instead of QPSK. In the QAM-DCSK, the QAM modulation is combined with the DCSK in a way so that the DCSK orthogonal channels are used to carry the in-phase and quadrature phase of the QAM signal. In the

HE-DCSK, the two bits are carried in one data modulated sequence by recycling each reference slot. All these techniques adding a complexity to the design when compared to the DCSK. Another drawback in the DCSK design is the weakened data security since the reference slot and information bearing slot are of an identical frequency analysis, this problem is fixed in [16], by adding a permutation mapping after the DCSK signal and scrambling the sequence that will break down the similarity between the information carrier signals and the reference. In [17, 18], Code shifted DCSK (CS-DCSK) and CS-QCSK, respectively, are proposed to fix the weakness of the broadband delay component in the DCSK using the Walsh code that allows both the data bearing signal and reference signal joined together in the same slot. An extended scheme to CS-DCSK is studied in [19], namely a high data-rate code shifted HCS-DCSK in which chaotic sequences with unlike initial conditions are used instead of the Walsh sequences to separate distinct information. These later techniques increase the information rate but require a synchronization technique, which affects the DCSK structure, at the receiver side. Another drawback of the DCSK is the duplication of the chaotic signal which slows the information rate and wastes the bit energy. In [20–22] phase separated PS-DCSK, improved I-DCSK, and short references SR-DCSK, respectively, are designed to enhance this weakness. In PS-DCSK, the symbol duration of the transmitted signal is reduced to a half by separating the reference chaotic signals from the information carrier signals using I and Q channels. I-DCSK is another approach to reducing the symbol duration to a half by adding the reference chaotic signals to the information carrier signals after the time reversal. The frame length of the transmitted signal in the SR-DCSK is minimized by generating the information bearing sequence from the R samples of the reference sequence and then duplicated P times to become the frame duration PR+R) samples. Therefore, it is only needed to generate R samples of the reference signal without a change of the received bit energy. Another drawback of the DCSK is a performance degradation in a fast fading channel, in [23], a continuous mobility DCSK (CM-DCSK) is designed to enhance the performance of the DCSK over a fast fading channel without a channel estimation. It uses a one-chip period delay for each sequence instead of a delay with β samples. This technique increases the strength of the system to a rapid variation of the channel parameters during the overall transmitter symbol duration. The Frequency Modulation (FM) combined with the QCSK system, which is named FM-QCSK, enhances the variation of the amplitude of the chaotic signal and the bandwidth efficiency. Furthermore, different studies were proposed in the last years to enhance the DCSK communication system as demonstrated in [24–27].

In this paper, we used a short reference quadrature chaos shift keying, the reference signal length in it is reduced to R samples in the same way as the SR-DCSK in [22] with the following differences:

(1.) Short reference QCSK system is designed and performance analysis is represented.

(2.) Evaluating the data-rate and energy saving improvement, compared to conventional QCSK and DCSK systems.

(3.) Drive the theory performance of SR-QCSK in AWGN and multipath Rayleigh fading channels.

(4.) Comparing SR-QCSK with other techniques of DCSK including DCSK, HE-DCSK, I-DCSK, NR-DCSK, PS-DCSK, SR-DCSK and CS-DCSK.

(5.) Comparing the effect of a different chaotic map on the SR-QCSK performance.

The rest of the paper is structured as follows: the QCSK system is briefly introduced and a block diagram of the SR-QCSK is demonstrated in section 2. Section 3 contains the performance analysis of the SR-QCSK system. In section 4, simulation results are presented and the conclusions are presented in section 5.

2. Quadrature chaos shift keying systems

2.1. Conventional QCSK communication system

In the first of the QCSK systems, a bits-to-symbol converter is used to map each two bits $d_j d_{j+1} = \{00, 11, 10, 01\}$ into the corresponding four phase constellation symbol $a_m + i\, b_m = \{(1+i), (-1-i), (-1+i), (1-i)\}$ in the same manner as in the quadrature phase shift keying (QPSK). This symbol is then transmitted using the QCSK modulator [12, 23] in which two sets of chaotic sequences put in two time slots of the same length in the same scenario as the DCSK system but the difference here is to carry a complex symbol instead of a bit. In the first time slot, the reference chaotic signal is placed while the second time slot contains the information carrier signals where the real and imaginary parts of the symbol are located in the same slot and separated by using orthogonal chaotic sequences. The separation is presented by adding the duplication of the chaotic reference multiplied by the real part of the m^{th} symbol with that of the orthogonal chaotic that is multiplied by the imaginary part of the m^{th} symbol. The orthogonal chaotic sequence is generated by taking the Hilbert transform to the reference-sequence, where the $\pi/2$ phase shift is created in every frequency component. In the digital domain, the Hilbert transform is generated either by taking the fast Fourier transform (FFT), eliminating the negative frequency coefficients and then taking the inverse FFT, or by using a digital filter design [28]. Let's define 2β as the number of the spreading sequence that is transmitted for each information symbol, called the spreading factor, where β is an integer number and $T_{QCSK} = 2\,\beta\,T_c$ is the QCSK symbol's duration, where T_c is the spreading time. The QCSK sequence of the m^{th} sample and the k^{th} spreading signal $s_{k,m}$, is given by:

$$s_{k,m} = \\ = \begin{cases} x_{k,m} & \text{for } 0 < k < \beta \\ \frac{1}{\sqrt{2}}\left(a_m x_{k-\beta,m} + b_m \tilde{x}_{k-\beta,m}\right) & \text{for } \beta < k \leq 2\beta \end{cases} \tag{1}$$

where $x_{k,m}$ is the reference-sequence, $x_{k-\beta,m}$ is $x_{k,m}$ the signal delayed by β value and $\tilde{x}_{k-\beta,m}$ is the orthogonal chaotic signal created by the Hilbert transform. Furthermore, the bit energy of the QCSK transmitter is $E_{b,m} = \beta E\left[x^2_{k,m}\right]$ where $E[.]$ is the expectation value of the corresponding signal. The information bits are detected by correlating the information carrier part of the received sequence with the chaotic basis sequences $x_{k,m}$ and $\tilde{x}_{k,m}$ over the βT_c duration and then comparing the results to a zero threshold. The received bit energy after the detection must be designed to be equal to $\beta E[x^2_{k,m}]/2$. The transmitter and receiver block diagram of the QCSK system is illustrated in figure 1.

2.2. Proposed SR-QCSK design system

The data-rate and energy efficiency of the QCSK system is decreased because a half of the bit duration contains the reference sequence without carrying any information. To enhance the QCSK system, the short reference algorithm is adopted with the QCSK to generate the SR-QCSK in a similar scenario of the SR-DCSK [22]. Figure 2a shows the scheme diagram of the SR-QCSK modulator. Firstly, each two bits are converted to a complex symbol using bit-to-symbol mapping. For each m^{th} symbol $a_m + i\,b_m$, a chaotic reference signal with the length R is produced and used and put in the first slot. The reference signal is repeated P times and these sequences are used as data-carrier sequences that consist of $P \cdot R$ samples. The information carrier sequences are put in the second slot and consist of adding two signals. In the first, the real m^{th} sample a_m is multiplied by the duplicated reference sequences to produce a signal of a length β where $\beta = P{\cdot}R$, while the 2^{nd} signal has the imaginary m^{th} sample that is multiplied by the P replicas of the Hilbert transform of the reference signal. These two sequences are added together to produce a data-carrier sequence with β samples. The SR-QCSK signal of the m^{th} sample and the k^{th} spreading signal $s_{k,m}$, is given by:

$$s_{k,m} = \\ = \begin{cases} x_{k,m} & \text{for } 0 < k \leq R \\ \frac{1}{\sqrt{2}}\left(a_m x_{k-R,m} + b_m \tilde{x}_{k-R,m}\right) & \text{for } R < k \leq \dots \\ & \cdots \leq (1+P)R \end{cases}$$

$$\text{and } x_{k-R,m} \equiv x_{0,m}, \quad \tilde{x}_{k-R,m} \equiv \tilde{x}_{0,m} \bmod(R) \tag{2}$$

Figure 2d illustrates a block diagram of the SR-QCSK demodulator. The received sequence $r_{k,m}$ is a complex signal where the reference sequence is extracted from the first slot of the SR-QCSK frame. We need two correlations to recover two bits. The 1^{st} correlation correlates the conjugate of the received reference sequence with the length R over P consecutive signals of the frame. The P correlations are then adding together to get:

$$C_{1,m} = T_c \sum_{p=0}^{p-1} \sum_{k=0}^{R-1} r^*_{k,m} r_{k+(1+P)R,m} \tag{3}$$

where $r^*_{k,m}$ is the conjugate of the received reference signal and $r_{k+(1+P)R,m}$ are the received data-carrier sequences. In the second correlator, the Hilbert transform is carried out first for the reference signal, before the correlation occurs, which results in:

$$C_{2,m} = T_c \sum_{p=0}^{p-1} \sum_{k=0}^{R-1} \tilde{r}^*_{k,m} r_{k+(1+P)R,m} \tag{4}$$

where $\tilde{r}^*_{k,m} = (\mathcal{H}(r_{k,m}))$ is the conjugate of the Hilbert transform of the received reference sequence and $\mathcal{H}(.)$ is the Hilbert transform function. The real and imaginary components of the m^{th} symbols are then estimated by comparing the real components of $C_{1,m}$ and $C_{2,m}$ to establish the threshold. Finally, the symbol to bit converter converts the symbol decision into stream bits.

3. Design and analysis of SR-QCSK systems

3.1. Information-rate and energy saving enhancement factor

Minimizing the length of the frame will enhance both the information rate and the energy bit of the transmitted signal. The derivation of the enhancement factor for the SR-QCSK system can be deduced in the same scenario as in [22], where the enhancement factor of the information-rate and energy saving is derived for the SR-DCSK relative to the DCSK system. Let us define $T_{b,SR-QCSK} = R + \beta T_c/2$, $T_{b,QCSK} = \beta T_c$ and $T_{b,DCSK} = 2\beta T_c$ as the SR-QCSK, QCSK and DCSK bit duration respectively. Then, the SR-QCSK information-rate enhancement factors IRE1 and IRE2, compared to QCSK and DCSK, respectively, are written in a percentage form as:

$$\text{IRE1} = \left(\frac{T_{b,QCSK}}{T_{b,SR-QCSK}} - 1\right) \times 100\% = \frac{\beta - R}{\beta + R} \times 100\% \tag{5}$$

$$\text{IRE2} = \left(\frac{T_{b,DCSK}}{T_{b,SR-QCSK}} - 1\right) \times 100\% = \frac{3\beta - R}{\beta + R} \times 100\% \tag{6}$$

From Eq. 5, it can be seen that the IRE1 is the same information-rate enhancement factor as the one

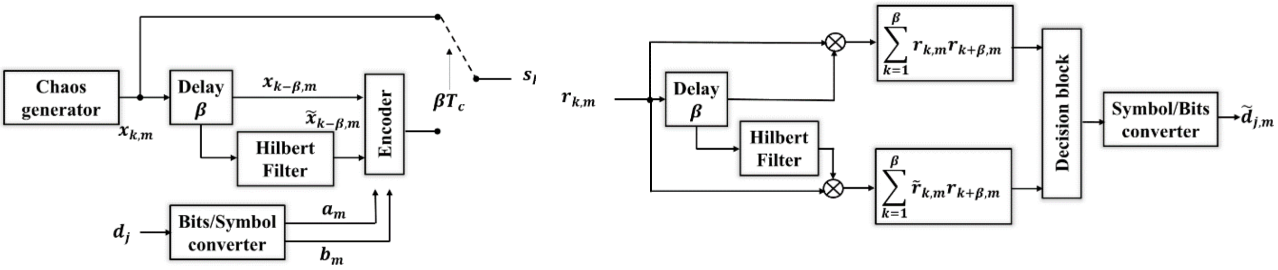

(A) . QCSK transmitter.　　　(B) . QCSK receiver.

Figure 1. Block diagram of the QCSK system.

of the SR-DCSK relative to the DCSK [22]. In a similar way, the energy-saving enhancement factors ESE1 and ESE2 for the SR-QCSK, relative to the QCSK and the DCSK, respectively, are calculated in a percent form as:

$$\text{ESE1} = \left(1 - \frac{E_{b,SR-QCSK}}{E_{b,QCSK}}\right) \times 100\%$$

and

$$\text{ESE2} = \left(1 - \frac{E_{b,SR-QCSK}}{E_{b,DCSK}}\right) \times 100\% \tag{7}$$

Where $E_{b,SR-QCSK} = T_c(\beta + R)Ex_k^2)/2$, $E_{b,QCSK} = T_c\beta Ex_k^2$ and $E_{b,DCSK} = 2T_c\beta Ex_k^2$ represents the energy bit of the SR-QCSK, QCSK and DCSK systems, respectively, at the transmitter side. The ESE1 and ESE2 are rewritten as:

$$\text{ESE1} = \frac{\beta - R}{2\beta} \times 100\%$$

and

$$\text{ESE2} = \frac{3\beta - R}{4\beta} \times 100\% \tag{8}$$

Eq. 8 proves that the ESE of the SR-QCSK, relative to the QCSK, is identical to that of the SR-DCSK relative to the DCSK, which is discussed in [22]. Figure 3 shows the percentage of the IRE and ESE of the SR-QCSK versus R samples for $\beta = 100$. It can be seen that, for the IRE1 and IRE2 curve when $R = 0$, the enhancement reaches the maximum value of 100 % and 300 %, when compared to the QCSK and DCSK, respectively. This means that the SR-QCSK system increased the information rate twofold, compared to the QCSK, and sixfold, when compared to the DCSK. When $R = \beta$, the SR-QCSK becomes the same as of the QCSK IRE1 = 0 % and IRE2 = 100 %. Similarly, for the ESE1 and ESE2 curves, the energy saving enhancement factor ranges from 50 % - 100 % and 75 % - 50 %, when compared to the QCSK and DCSK, respectively.

3.2. BER analytic performance of SR-QCSK system

In this section, the BER performance of the SR-QCSK is analytically derived over the AWGN and a multipath slow Rayleigh fading channel. The chaotic signal is generated using the second order Chebyshev polynomial function (CPF) with a unity variance and zero mean [29].

$$x_{k+1} = 1 - 2x_k^2 \tag{9}$$

A multipath fading channel with an L independent path number that is used in [2, 22] is considered. In this channel, τ_ℓ and α_ℓ are the ℓ^{th} path time delay and complex coefficient, respectively. Also, n_k is an additive white Gaussian noise with a variance equal to $N_0/2$ and zero mean. The channel coefficients α_ℓ are independent and of an identical Rayleigh distribution and considered to be fixed during the whole transmitted frame, this means that it is a slow fading channel with a probability density function (PDF) given by

$$f(\alpha) = \frac{\alpha}{\sigma^2} e^{\frac{\alpha^2}{2\sigma^2}} \tag{10}$$

where σ^2 is the variance of the received voltage signal. The discrete output of the L-tapped delay Rayleigh fading channel is written as

$$r_k = \sum_{\ell=1}^{L} \alpha_\ell s_{k-\tau_\ell} + n_k \tag{11}$$

where $s_{k-\tau_l}$ is the channel delay version of the sending signal $s_{k,m}$, where the letter index m is omitted for simplicity. To derive the bit error rate (BER) analysis of the SR-QCSK over the AWGN and multipath Rayleigh fading channel, first, it is assumed that the maximum channel delay τ_{max} is much less than the reference length R in which $0 < \tau_{max} \ll R$ [22, 30]. For simplicity, $T_c = 1$ and the index m is omitted from all analysis. Because the real and imaginary parts of the data are identical in detection, only the first correlation and decision is derived. By substituting Eqs. (2 and 11) into Eqs. (3 and 4), the received correlation output can be expressed as

$$C_1 = \sum_{p=0}^{p-1} \sum_{k=0}^{R-1} \left(\sum_{\ell=1}^{L} \left(\left(\frac{1}{\sqrt{2}} a\alpha_\ell x_{k+1+P)R-\tau_\ell} + \right.\right.\right.$$
$$\left.\left.\left. + \frac{1}{\sqrt{2}} b\alpha_\ell \tilde{x}_{k+1+P)R-\tau_\ell} \right) + n_{p,k+R} \right) \right)$$

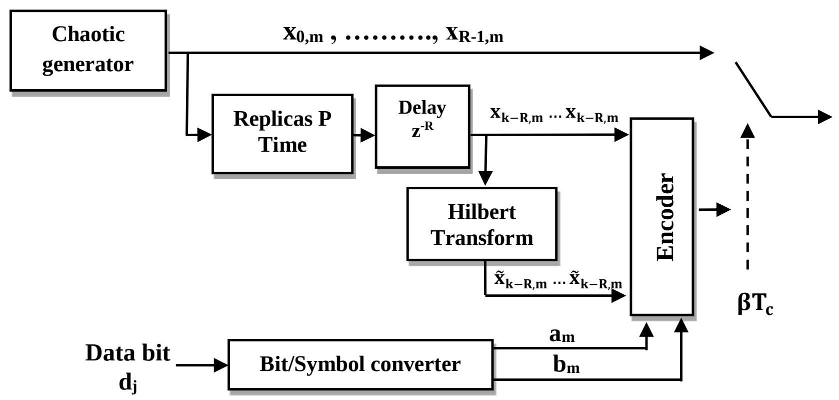

(a) . SR-QCSK modulator.

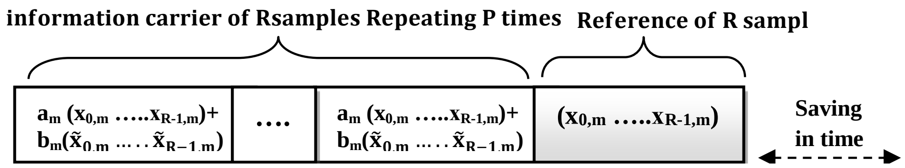

(b) . SR-QCSK frame.

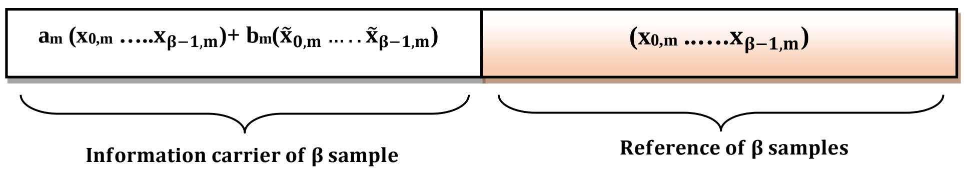

(c) . QCSK frame

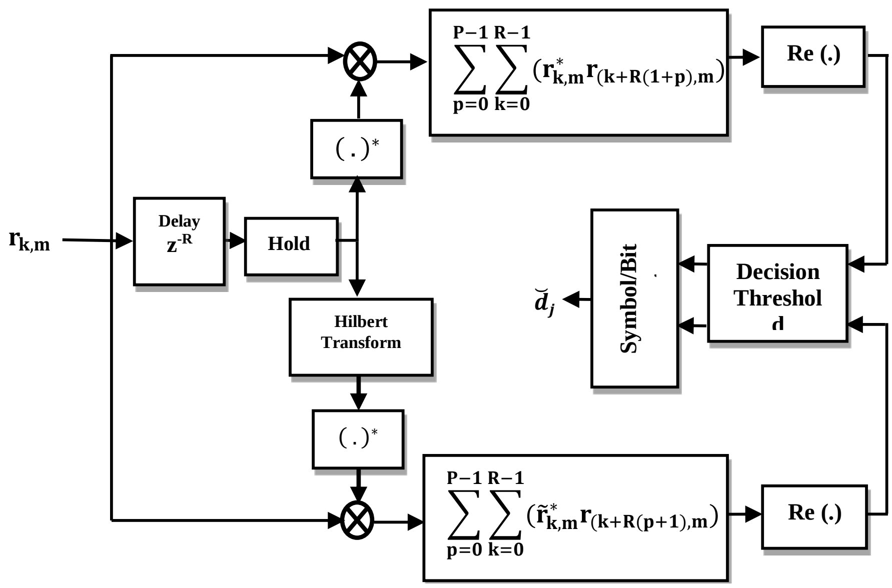

(d) . SR-QCSK demodulator.

Figure 2. a) The scheme of the SR-QCSK modulator, b) SR-QCSK frame, c) QCSK frame and d) SR-QCSK demodulator.

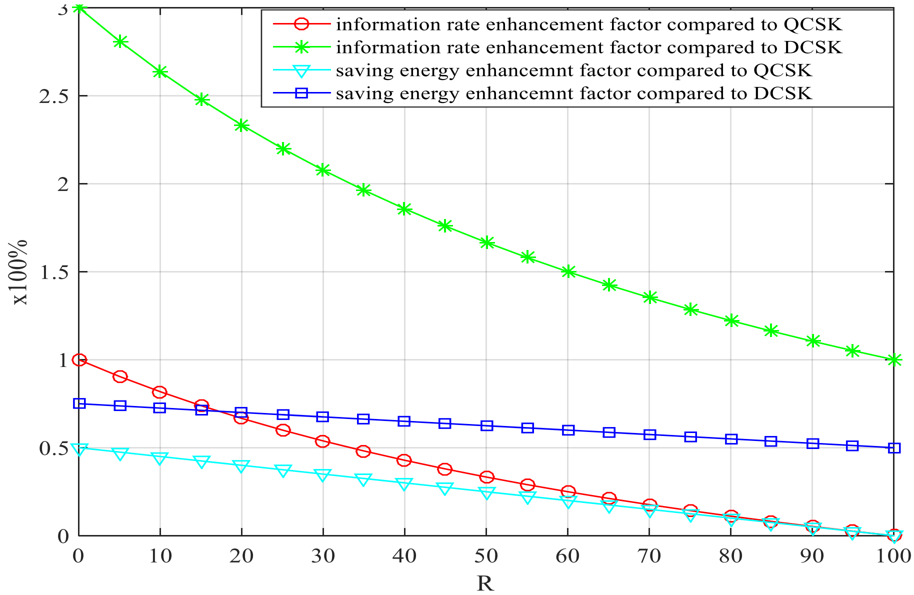

Figure 3. The percentage form of the information rate and saving energy enhancement of the SR-QCSK for $\beta = 100$.

$$\left(\sum_{\ell=1}^{L}\alpha_\ell x_k + n_k\right)^* \quad (12)$$

and

$$C_2 = \sum_{p=0}^{p-1}\sum_{k=0}^{R-1}\left(\sum_{\ell=1}^{L}\left(\left(\frac{1}{\sqrt{2}}a\alpha_\ell x_{k+1+P)R-\tau_\ell} + \frac{1}{\sqrt{2}}b\alpha_\ell \tilde{x}_{k+1+P)R-\tau_\ell}\right) + n_{p,k+R}\right)\right)\left(\mathcal{H}\left(\sum_{\ell=1}^{L}\alpha_\ell x_k + n_k\right)\right)^* \quad (13)$$

where $n_{p,k+R}$ is p^{th} Additive white Gaussian noise (AWGN) vector added to the p^{th} information sequence, n_k is the AWGN sequence that remains constant during all P correlations and $(.)^*$ is the conjugate operator. It can be noticed that the chaotic signal is periodic with period R, therefore, $x_{k+1+P)R-\tau_\ell} = x_{k-\tau_\ell}$ and x_k has the same sequence for each P correlations, also, for large value of R, the following expressions is approximated as [22].

$$\sum_{k=1}^{R} x_{k-\tau_\ell}x_{k-\tau_\mathcal{V}} \approx 0, \quad \ell \neq \mathcal{V} \quad (14)$$

And from the Hilbert transform property, the following expression is used [12]

$$\sum_{k=0}^{R-1} x_{k-\tau_\ell}\tilde{x}_{k-\tau_\ell} = 0 \quad (15)$$

From Eqs. 12-15, the first decision variable D_1 = Real C_1, and the second decision variable D_2 = Real C_2, that represent the input to the 1^{st} and 2^{nd} thresholding blocks respectively, are expressed as:

$$D_1 = \mathcal{R}e\left(P\sum_{k=0}^{R-1}\left(\frac{a}{\sqrt{2}}\sum_{\ell=1}^{L}|\alpha_\ell|^2 x^2_{k-\tau_\ell} + \frac{1}{\sqrt{2}}n_k^*\sum_{\ell=1}^{L}a\alpha_\ell x_{k-\tau_\ell} + b\alpha_\ell\tilde{x}_{k-\tau_\ell}\right) + \sum_{p=0}^{p-1}\sum_{k=0}^{R-1}\left(n_{p,k+R}n_k^* + n_{p,k+R}\sum_{\ell=1}^{L}\alpha_\ell x_{k-\tau_\ell}\right)\right) \quad (16)$$

and

$$D_2 = \mathcal{R}e\left(P\sum_{k=0}^{R-1}\left(\frac{b}{\sqrt{2}}\sum_{\ell=1}^{L}|\alpha_\ell|^2 \tilde{x}^2_{k-\tau_\ell} + \frac{1}{\sqrt{2}}\tilde{n}_k^*\sum_{\ell=1}^{L}a\alpha_\ell x_{k-\tau_\ell} + b\alpha_\ell\tilde{x}_{k-\tau_\ell}\right) + \sum_{p=0}^{p-1}\sum_{k=0}^{R-1}\left(n_{p,k+R}\tilde{n}_k^* + n_{p,k+R}\sum_{\ell=1}^{L}\alpha_\ell \tilde{x}_{k-\tau_\ell}\right)\right) \quad (17)$$

where $\mathcal{R}e(.)$ is the real part of the sequence, $\tilde{n}_k^*$ is the conjugate of $\tilde{n}_k$ and $\tilde{n}_k = \mathcal{H}(n_k)$ where, for an ideal Hilbert transform, it is matching with nk that is AWGN [12]. From the two equations above, the first term is due to the required data a and b, respectively, while the remaining expressions are due to the noise and interference signal.

From the central limit theorem, the decision variable is considered as Gaussian distribution. Therefore, the

BER of the SR-QCSK is expressed as

$$\begin{aligned}\mathrm{BER} = \frac{1}{4}\Pr\left(D_1 < 0|a = +1\right) + \\ + \frac{1}{4}\Pr\left(D_1 > 0|a = -1\right) + \frac{1}{4}\Pr\left(D_2 < 0|b = +1\right) + \\ + \frac{1}{4}\Pr\left(D_2 < 0|b = -1\right) \quad (18)\end{aligned}$$

Since each term in Eq. 18 is symmetric, the BER is calculated in terms of the complementary error function (erfc) and is given by:

$$\mathrm{BER} = \frac{1}{2}\mathrm{erfc}\left(\left[\frac{2VD_1}{ED_1^2}\right]^{-\frac{1}{2}}\right) \quad (19)$$

where $\mathrm{erfc}(z) = \frac{2}{\sqrt{\pi}}\int_z^\infty e^{-z^2}dz$, $V(.)$ and $E(.)$ are the variance and the mean value of the corresponding sequence. By assuming that E_b is constant for all transmitted symbols with a long duration R, write $E(x_k^2)$ in terms of bit energy E_b ($E(x_k^2) = 2E_b/R+\beta$), and substitute $a = +1$. The average of the decision variable D_1 is given as

$$E(D_1) = \frac{PR}{(R+\beta)}\sqrt{2}E_b\sum_{\ell=1}^{L}|\alpha_\ell|^2 \quad (20)$$

Since all terms in Eq. 16 are independent, the variance of the decision variable D_1 in terms of E_b is given by

$$\begin{aligned}V(D_1) = \frac{P^2R}{(R+\beta)}N_0\sum_{\ell=1}^{L}|\alpha_\ell|^2E_b + PR\frac{N_0^2}{4} + \\ + \frac{PR}{(R+\beta)}N_0\sum_{\ell=1}^{L}|\alpha_\ell|^2E_b \quad (21)\end{aligned}$$

If we substitute Eq. 20 and 21 into Eq. 19 and define $\gamma = \sum_{\ell=1}^{L}|\alpha_\ell|^2E_b/N_0$, then the conditional BER for the SR-QCSK system is given by:

$$\mathrm{BER} = \frac{1}{2}\mathrm{erfc}\left(\left[\frac{R+\beta}{R\gamma}\left(\frac{p+1}{p}\right) + \frac{R+\beta^2}{4RP\gamma^2}\right]^{-\frac{1}{2}}\right) \quad (22)$$

The average BER over the PDF of γ is calculated as:

$$\begin{aligned}\overline{\mathrm{BER}} = \frac{1}{2}\int_0^\infty \mathrm{erfc}\left(\left[\frac{R+\beta}{R\gamma}\left(\frac{p+1}{p}\right) + \right.\right. \\ \left.\left. + \frac{R+\beta^2}{4RP\gamma^2}\right]^{-\frac{1}{2}}\right) f(\gamma)d\gamma \quad (23)\end{aligned}$$

where $f(\gamma)$ is the pdf of γ that is expressed as [22]

$$f(\gamma) = \sum_{\ell}^{L}\frac{1}{\overline{\gamma}_\ell}\left(\prod_{j=1,\, j\neq\ell}^{\ell}\frac{\overline{\gamma}_\ell}{\overline{\gamma}_\ell - \overline{\gamma}_j}\right)e^{-\frac{\gamma}{\overline{\gamma}_\ell}} \quad (24)$$

where $\overline{\gamma}_\ell$ is the expectation value of $\gamma_\ell = |\alpha_\ell|^2E_b/N_0$ which is the ℓ^{th} instantaneous signal-to-noise ratio Eq. 25 is calculated for a set of classes here 1000 set is taken) using numerical integration with unit integration step size [22]. Moreover, the BER of the SR-QCSK over the AWGN can be calculated from Eq. 24. By defining $\sum_{\ell=1}^{L}|\alpha_\ell|^2 = 1$ and assuming R is large, we get the following

$$\begin{aligned}\mathrm{BER}_{\text{SR-QCSK}} = \frac{1}{2}\mathrm{erfc}\left(\left[\frac{(R+\beta)N_0}{RE_b}\left(\frac{p+1}{p}\right) + \right.\right. \\ \left.\left. + \frac{R+\beta^2N_0^2}{4RPE_b^2}\right]^{-\frac{1}{2}}\right) \quad (25)\end{aligned}$$

4. Simulation results and discussions

In this section, the simulation results and a comparison under the AWGN and multipath fading channel is presented. Matlab program 2015 is used in this simulation.

4.1. AWGN channel results

Figure 4 shows the BER performance SR-QCSK over the AWGN channel for $P = 1, 2$, and 4 when $\beta = 100$. The performance is also compared with the DCSK system. As can be seen from this figure, the simulation performance follows the analytic expression given in Eq. 25. In [22], the relation for an optimal value of R named R_{opt} is derived for the SR-DCSK system and it is proven that R_{opt} depends on E_b/N_0 and reaches optimal values when $R = 50$ for $\beta = 100$. From this figure it can be seen that the best BER performance is obtained when $P = 2$. In a similar way, Figure 4 shows the optimal performance of the SR-QCSK system for $R = 50$, this performance is superior to any other results. Also when $R = 25$, there is a little difference in performance as compared to QCSK and its performance being better than the one of the DCSK. According to Eqs. 5, 6 and 8, when $R = 25$ or $R = 50$, the SR-QCSK enhanced the information rate by 60 % and 33 %, respectively, in comparison to the QCSK system, and by 220 % and 166 %, respectively, in comparison to the DCSK system. Also, the energy saving is enhanced by 37 % and 25 % in comparison to the QCSK and enhanced by 68 % and 62 % in comparison to the DCSK for $R = 25$ and 50, respectively.

Figure 5 shows the BER performance of the SR-QCSK for $\beta = 50$, 100,and 200 when $P = 2$ and compares the results with the QCSK $P = 1$). It can be seen that doubled β will degrade the E_b/N_0 gain by a factor less than 1 dB, since increasing β will increase the noise power at the same time. Also, a short reference technique enhances the information rate of QCSK by 33 % and 166 % in comparison to the QCSK and DCSK, respectively. And it enhanced the saving energy by 25 % and 62 % in comparison to the QCSK and DCSK, respectively, when $R = \beta/2$ with the BER performance being better than the one of the QCSK system.

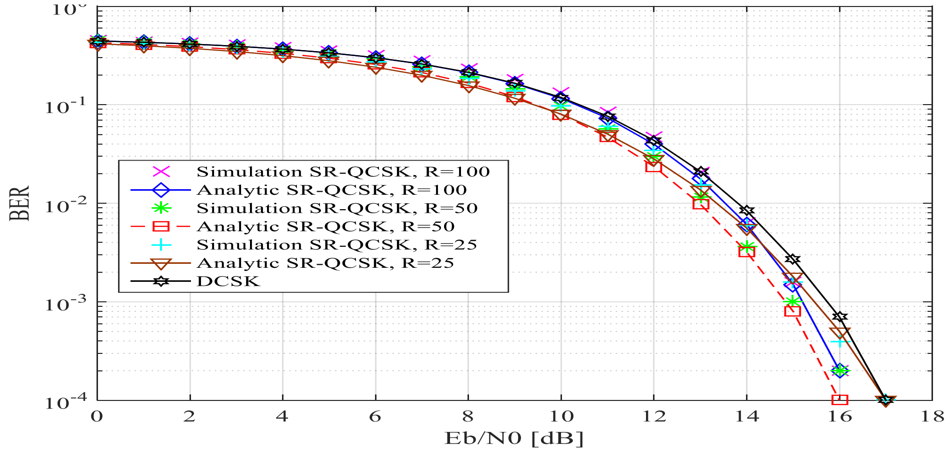

Figure 4. The BER performance analysis and simulation of the SR-QCSK over the AWGN channel for $P.R = 100$ and $R = 100$, 50 and 25.

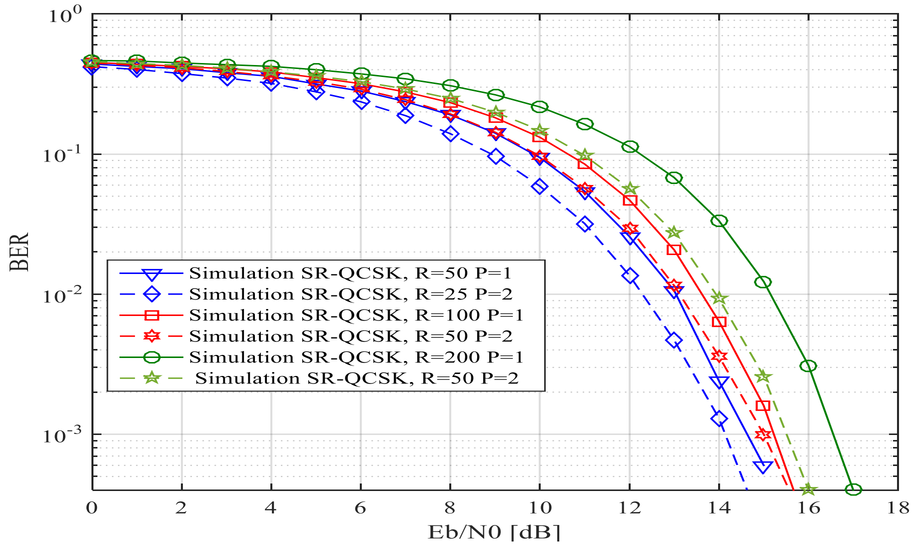

Figure 5. Simulated BER performance of the SR-QCSK under the AWGN channel for $P = 2$ and $P.R = 50$,100 and 200.

In Figure 6, the SR- QCSK for $P = 2$ is compared with different families of the DCSK system, including the DCSK, HE - DCSK, I-DCSK, NR-DCSK, PS-DCSK, SR-DCSK and CS-DCSK for $\beta = 100$. The SR-QCSK has a better performance than the DCSK, HE-DCSK, SR-DCSK, PS-DCSK and CS-DCSK, while it's E_b/N_0 gain lowered by about 0.8 dB and 1.3 dB at BER $= 10^{-3}$ in comparison to the I-DCSK and NR-DCSK, respectively, over the AWGN channel. Notice that, in NR-DCSK, $p = 5$ represents the number of the repeating chaotic sample and, in CS-DCSK, N represents the Walsh codes order.

4.2. Multipath Rayleigh fading channel results

In this simulation, two paths of the Rayleigh fading channel are considered with the same channel parameters used in [4]. The mean power in the two paths are $E(\alpha_1^2) = 2/3$ and $E(\alpha_2^2) = 1/3$ with corresponding delays for each path $\tau_1 = 0$ and $\tau_2 = 2T_c$ respectively. Figure 7 illustrates the BER performance of the SR-QCSK system under a multipath fading channel for $P.R = 100$ and for $P = 1$, 2 and 4. It can be seen that even though there are slight gaps between the analytic and simulation results, especially when R is decreased due to neglection of the inter symbol interference (ISI)($\tau \ll R$) the simulation follows the analytic BER results. From this figure, it can be seen that the SR-QCSK is robust against the multipath fading channel and does not need any information about the channel at the receiver. Also, For $R = 100$ and $P = 1$, the SR-QCSK is the same QCSK system.

The performance comparison of the SR-QCSK with different techniques of the DCSK, including DCSK, HE-DCSK, I-DCSK, NR-DCSK, PS-DCSK, SR-DCSK and CS-DCSK, for $\beta = 100$ is illustrated in Figure 8. It can be seen that the short reference technique has not only improved the information-rate and energy-saving of the system, but also improved the BER over all families of the DCSK mentioned here due

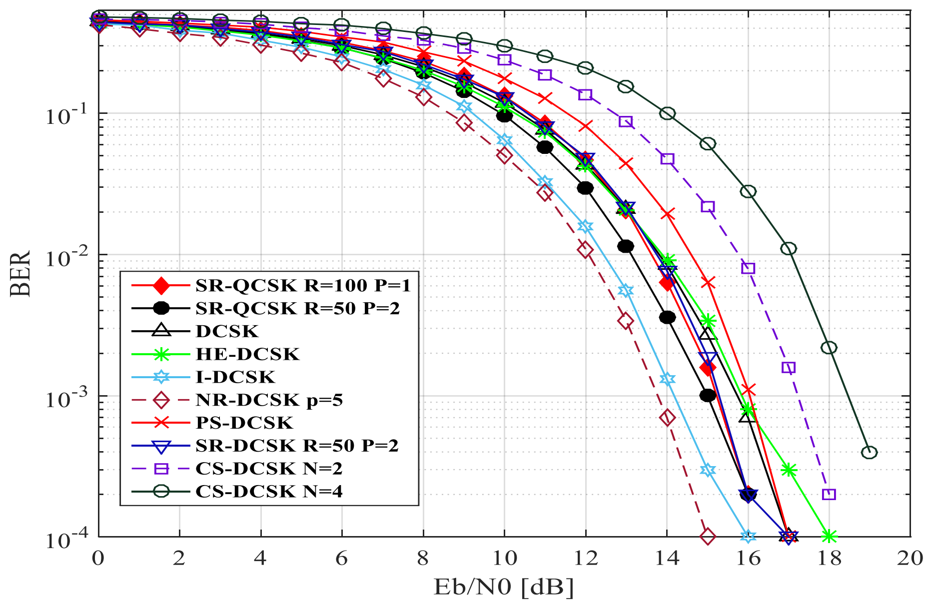

FIGURE 6. A comparison of the BER performance simulation with the SR-QCSK with different techniques of the DCSK for $P.R = 100$ in the AWGN channel.

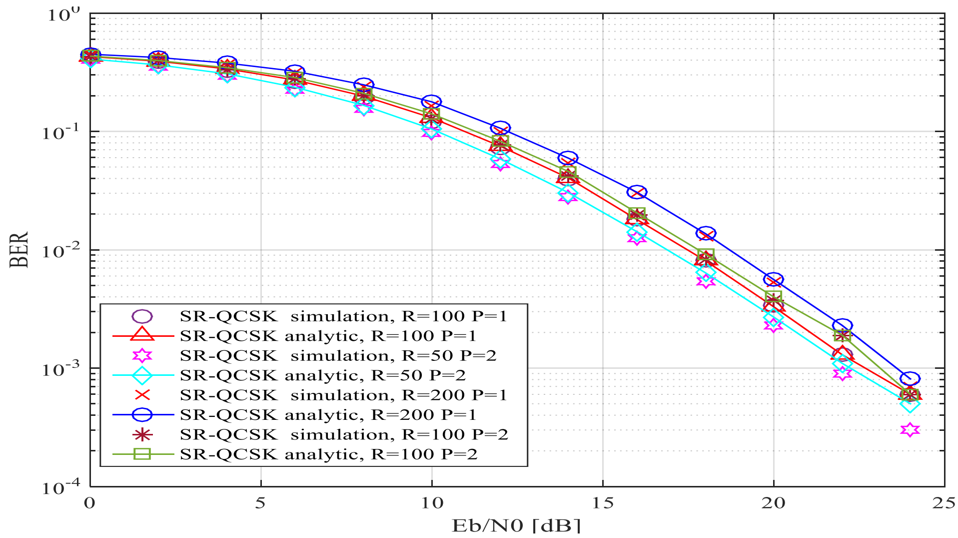

FIGURE 7. The BER performance of the SR-QCSK system under two paths of the Rayleigh fading channel for $P.R = 100$ and $P = 1$, 2 and 4.

to reduction of the reference chaotic length to R value. Also, the SR-QCSK has the best BER performance of all. Even though I-DCSK and NR-DCSK systems have a better BER performance than other techniques in the AWGN referred in Figure 7, the priority of the best BER performances are weaker in the multipath fading channel especially for the I-DCSK. The degradation of the performance of the I-DCSK is due to the reverse reference chaotic signal being added to the information-bearing signal, which causes an inter-symbol interference increase and the orthogonality to detect the transmitted data is missing. Table 1 shows the comparison of different techniques for E_b/N_0 at $\text{BER} = 10^{-3}$.

5. Conclusions

In this paper, a short-reference quadrature chaos- shift keying (SR-QCSK) is presented to enhance the data rate and to put a bit energy in a conventional QCSK without adding extra complexity in the transmitter or the receiver side or influence the BER performance. The main idea of the short reference technique is minimizing the length of the reference chaotic signal at the transmitter by a factor P and comparing the new to the original length to produce R reference sequences, while the length of the bearing information signal remains unchanged. This is done by duplicating the reference signal P times to get the same length as the conventional QCSK. Therefore, the symbol duration is reduced to $(R + \beta)T_c$ instead of $2\beta T_c$. This reduction will improve the data rate, energy saving

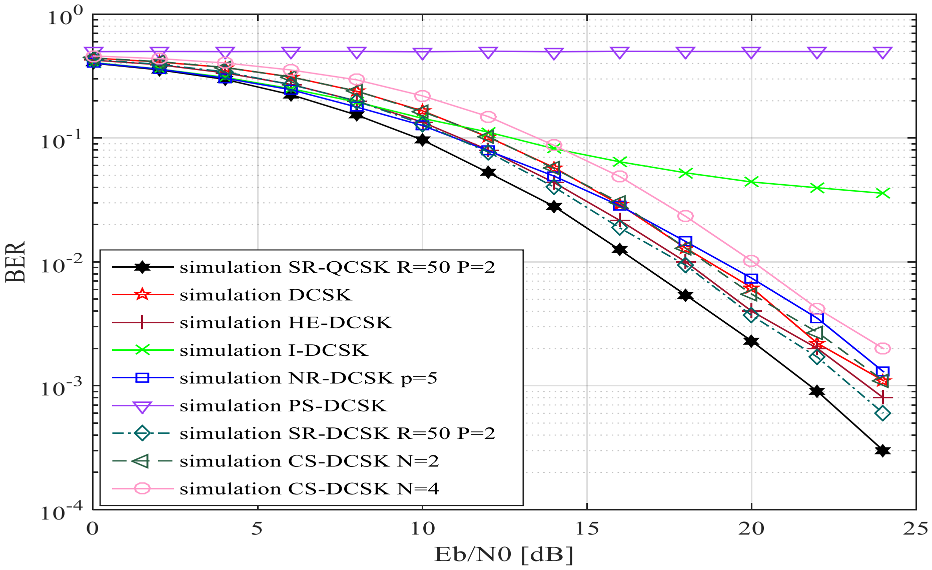

Figure 8. A comparison of the BER performance simulation with the SR-QCSK with different techniques of the DCSK for $P.R = 100$ over a multipath fading channel.

Channel/Method	Proposed	DCSK	SR-DCSK	HE-DCSK	CS-DCSK
AWGN	15	15.8	15.2	15.8	16.6
Multipath fading channel	22	24	23	23.5	24

Table 1. E_b/N_0 comparison of different techniques under the AWG and multipath fading channel.

per bit and BER performance in comparison to the conventional QCSK and DCSK. The energy saving enhancement factor and the information rate are derived by a comparison to the traditional QCSK and DCSK systems. When $R = 25$ or $R = 50$, it can be seen that the SR-QCSK enhanced the information rate by 60 % and 33 %, respectively, in comparison to the QCSK system and by 220 % and 166 %, respectively, in comparison to the DCSK system. The BER analytical expression of the SR-QCSK in multipath Rayleigh fading and AWGN channels are also derived and compared with computer simulation results. The results show that the theory and simulation are in an agreement. Furthermore, the SR-QCSK system is compared with other DCSK techniques in the AWGN and multipath fading channel. In AWGN, the performance is superior to the DCSK, HE-DCSK, SR-DCSK, PS-DCSK and CS-DCSK by about 0.8 dB, 0.4 dB, 1 dB and 2 dB, respectively, at BER $= 10^{-3}$ while it's E_b/N_0 gain decreased by about 0.8 dB and 1.3 dB at BER $= 10^{-3}$ in comparison to the I-DCSK and NR-DCSK, respectively. Also, the results of the multipath fading channel show that the SR-QCSK is superior to all DCSK techniques mentioned here, having a gain of about 1 dB over the SR-DCSK at BER $= 10^{-3}$. The SR-QCSK shows a good promise to be the one of the superior techniques in non-coherent differential chaos shift keying systems.

Acknowledgements

The authors would like to gratefully acknowledge the support of the Mustansiriyah University Baghdad Iraq (`www.uomustansiriyah.edu.iq`).

References

[1] G. Kaddoum. Wireless chaos-based communication systems: A comprehensive survey. *IEEE Access* **4**:2621 – 2648, 2016. doi:10.1109/ACCESS.2016.2572730.

[2] F. Lau, C. Tse. *Chaos-Based Digital Communication Systems*. Springer-Verlag, New York, 2003. doi:10.1007/978-3-662-05183-2.

[3] A. P. Kurian, S. Puthusserypady, S. M. Htut. Performance enhancement of DS/CDMA system using chaotic complex spreading sequence. *IEEE Transactions on Wireless Communications* **4**(3):984 – 989, 2005. doi:10.1109/TWC.2005.847028.

[4] Y. Xia, C. K. Tse, F. C. M. Lau. Performance of differential chaos-shift-keying digital communication systems over a multipath fading channel with delay spread. *IEEE Transactions on Circuits and Systems II: Express Briefs* **51**(12):680 – 684, 2004. doi:10.1109/TCSII.2004.838329.

[5] J. Yu, Y.-D. Yao. Detection performance of chaotic spreading LPI waveforms. *IEEE Transactions on Wireless Communications* **4**(2):390–396, 2005. doi:10.1109/TWC.2004.842948.

[6] M. Z. Hasan, I. Idris, A. F. M. N. Uddin, M. Shahjahan. Performance analysis of a coherent chaos-shift keying technique. In *15th International Conference*

on Computer and Information Technology (ICCIT), pp. 249 – 254. 2012. doi:10.1109/ICCITechn.2012.6509721.

[7] G. Kolumbán, B. Vizvári, W. Schwarz, A. Abel. Differential chaos shift keying: A robust coding for chaos communication. In *Proc. International Workshop on Non-linear Dynamics of Electronic Systems NDES, Seville, Spain*, pp. 92 – 97. 1996.

[8] Z. Zhou, J. Wang, Y. Ye. Exact BER analysis of differential chaos shift keying communication system in fading channels. *Wireless Personal Communications* **53**(2):299 – 310, 2010. doi:10.1007/s11277-009-9685-4.

[9] G. Kaddoum, F. Gagnon, P. Chargé, D. Roviras. A generalized BER prediction method for differential chaos shift keying system through different communication channels. *Wireless Personal Communications* **64**(2):425 – 437, 2012. doi:10.1007/s11277-010-0207-1.

[10] G. Kolumban, M. P. Kennedy, G. Kis, Z. Jako. FM-DCSK: a novel method for chaotic communications. In *Proceedings of the 1998 IEEE International Symposium on Circuits and Systems*, vol. 4, pp. 477 – 480. 1998. doi:10.1109/ISCAS.1998.698936.

[11] M. P. Kennedy, G. Kolumban, G. Kis, Z. Jako. Performance evaluation of FM-DCSK modulation in multipath environments. *IEEE Transactions on Circuits and Systems I: Fundamental Theory and Applications* **47**(12):1702 – 1711, 2000. doi:10.1109/81.899922.

[12] Z. Galias, G. M. Maggio. Quadrature chaos-shift keying: theory and performance analysis. *IEEE Transactions on Circuits and Systems I: Fundamental Theory and Applications* **48**(12):1510 – 1519, 2001. doi:10.1109/TCSI.2001.972858.

[13] H. Yang, G. Jiang. High-efficiency differential-chaos-shift-keying scheme for chaos-based noncoherent communication. *IEEE Transactions on Circuits and Systems II: Express Briefs* **59**(5):312 – 316, 2012. doi:10.1109/TCSII.2012.2190859.

[14] G. Zhang, Y. Wang, T.-q. Zhang. A novel QAM-DCSK secure communication system. In *7th International Congress on Image and Signal Processing*, pp. 994 – 999. 2014. doi:10.1109/CISP.2014.7003924.

[15] L. Wang, G. Cai, G. R. Chen. Design and performance analysis of a new multiresolution m-ary differential chaos shift keying communication system. *IEEE Transactions on Wireless Communications* **14**(9):5197 – 5208, 2015. doi:10.1109/TWC.2015.2434820.

[16] F. C. M. Lau, K. Y. Cheong, C. K. Tse. Permutation-based DCSK and multiple-access DCSK systems. *IEEE Transactions on Circuits and Systems I: Fundamental Theory and Applications* **50**(6):733 – 742, 2003. doi:10.1109/TCSI.2003.812616.

[17] W. K. Xu, L. Wang, G. Kolumbán. A novel differential chaos shift keying modulation scheme. *International Journal of Bifurcation and Chaos* **21**(03):799 – 814, 2011. doi:10.1142/S0218127411028829.

[18] K. Thilagam, K. Jayanthi. A novel chaos based modulation scheme (CS-QCSK) with improved BER performance. *Computer Science & Information Technology* pp. 45 – 59, 2012. doi:10.5121/csit.2012.2406.

[19] G. Kaddoum, F. Gagnon. Design of a high-data-rate differential chaos-shift keying system. *IEEE Transactions on Circuits and Systems II: Express Briefs* **59**(7):448 – 452, 2012. doi:10.1109/TCSII.2012.2198982.

[20] H. Yang, G. Jiang, J. Duan. Phase-separated DCSK: A simple delay-component-free solution for chaotic communications. *IEEE Transactions on Circuits and Systems II: Express Briefs* **61**(12):967 – 971, 2014. doi:10.1109/TCSII.2014.2356914.

[21] G. Kaddoum, E. Soujeri, C. Arcila, K. Eshteiwi. I-DCSK: An improved noncoherent communication system architecture. *IEEE Transactions on Circuits and Systems II: Express Briefs* **62**(9):901 – 905, 2015. doi:10.1109/TCSII.2015.2435831.

[22] G. Kaddoum, E. Soujeri, Y. Nijsure. Design of a short reference noncoherent chaos-based communication systems. *IEEE Transactions on Communications* **64**(2):680 – 689, 2016. doi:10.1109/TCOMM.2015.2514089.

[23] Y. Zhang, X. Shen, Y. Ding. Design and performance analysis of an FM-QCSK chaotic communication system. In *International Conference on Wireless Communications, Networking and Mobile Computing*, pp. 1 – 4. 2006. doi:10.1109/WiCOM.2006.198.

[24] Y. Zhang, X. Shen, Y. Ding. Design and performance analysis of an FM-QCSK chaotic communication system. In *International Conference on Wireless Communications, Networking and Mobile Computing*, pp. 1–4. 2006. doi:10.1109/WiCOM.2006.198.

[25] S. Kim, J. Bok, H. Ryu. Performance evaluation of DCSK system with chaotic maps. In *The International Conference on Information Networking 2013*, pp. 556 – 559. 2013. doi:10.1109/ICOIN.2013.6496686.

[26] F. S. Hasan. Design and analysis of an OFDM-based short reference quadrature chaos shift keying communication system. *Wireless Personal Communications* **96**(2):2205 – 2222, 2017. doi:10.1007/s11277-017-4293-1.

[27] F. S. Hasan, A. A. Valenzuela. Design and analysis of an OFDM-based orthogonal chaotic vector shift keying communication system. *IEEE Access* **6**:46322 – 46333, 2018. doi:10.1109/ACCESS.2018.2862862.

[28] A. V. Oppenheim, R. W. Schafer. *Discrete-Time Signal Processing*. Pearson, Boston, 3rd edn., 2010.

[29] G. Kaddoum, P. Chargé, D. Roviras, D. Fournier-Prunaret. A methodology for bit error rate prediction in chaos-based communication systems. *Circuits, Systems and Signal Processing* **28**(6):925 – 944, 2009. doi:10.1007/s00034-009-9124-5.

[30] H. Yang, W. K. S. Tang, G. Chen, G. Jiang. System design and performance analysis of orthogonal multi-level differential chaos shift keying modulation scheme. *IEEE Transactions on Circuits and Systems I: Regular Papers* **63**(1):146 – 156, 2016. doi:10.1109/TCSI.2015.2510622.